**Magnesium Technology 2011**
*Edited by: Wim H. Sillekens, Sean R. Agnew, Neale R. Neelameggham, and Suveen N. Mathaudhu*
*TMS (The Minerals, Metals & Materials Society), 2011*

# Effect of Fiber Reinforcement on Corrosion Resistance of Mg AM60 Alloy-based Composites in NaCl Solutions

Qiang Zhang, Henry Hu
Mechanical, Automotive & Materials Engineering
University of Windsor, 401 Sunset Ave.
Windsor, Ontario, Canada N9B 3P4
E-mail: qiangz@uwindsor.ca, huh@uwindsor.ca

## ABSTRACT

There is great interest in developing low-cost, magnesium-based MMCs because of their high stiffness-to-weight ratio for aerospace and automotive applications. However, corrosion resistance of metal-matrix composites is often a concern for components to be used in harsh environment. In this study, the corrosion behavior of $Al_2O_3$ fibres reinforced magnesium AM60 composite, in aqueous solutions containing various concentrations of NaCl, was studied in comparison to that of matrix AM60 alloy by potentiodynamic polarization measurements. The microstructure of the composite and matrix alloy AM60 before and after corrosion testing was analyzed by optical microscopy, and scanning electron microscopy (SEM). The results show that the presence of $Al_2O_3$ fiber deteriorates the corrosion resistance of the matrix magnesium alloy AM60. The effect of $Al_2O_3$ fiber reinforcement and NaCl concentrations on the corrosion behavior of the composites are discussed. The corrosion mechanisms of the composite are proposed in light of metallographic observation on the formation of corrosion products.

## INTRODUCTION

The need for high-performance and lightweight materials in automobile and aerospace industries has led to extensive research and development efforts generating metal matrix composites (MMCs) and cost-effective fabrication technologies. Magnesium-based composite materials allow constituent variation such that the properties of the materials can be tailored. Compared to the unreinforced monolithic metal, magnesium-based composites have been recognized to possess superior mechanical properties, such as high elastic modulus and strengths as well as enhanced wear resistance [1].

Extensive studies on mechanical properties and solidification behaviors of light metals and their composites have been carried out. Light metal-based composites are often fabricated by various manufacturing processes such as high pressure die casting, stir mixing, pressure infiltration and squeeze casting. Among the available techniques for manufacturing magnesium-based composites, preform-squeeze casting technique is considered to be an effective process. This is because it offers low cost, high efficiency, and uniform distribution of reinforcements to the fabrication of the composites, in which different volumes, especially relatively low volumes, of reinforcements are required [1-5]. Since magnesium alloys possess a very active behavior in moist environment, addition of an appropriate reinforcement into metal matrix which improves physical and mechanical properties often deteriorates the corrosion resistance of composites.

However, relatively scarce investigation about corrosion behavior of $Al_2O_3$ reinforced magnesium based composites, in particular under aggressive environments, is performed. In this study, the influence of $Al_2O_3$ fiber on the corrosion behavior of $Al_2O_3$/AM60 composites, obtained by preform-squeeze casting, was evaluated in aqueous solutions containing various concentrations of NaCl by electrochemical experimentation and microstructure analysis.

## EXPERIMENTAL PROCEDURE

### Composites preparation

$Al_2O_3$ short fibres were employed as the raw materials for preparation of reinforcements since they are relatively inexpensive and possess adequate properties. The matrix alloy was magnesium alloy AM60 with the chemistry composition (wt%) of 6.0Al-0.22Zn-0.4Mn-0.1Si-0.01Cu-0.004Fe-0.002Ni-Mg due to its wide usage in the automotive industry. The thermophysical properties of the $Al_2O_3$ fibre as well as the matrix alloy (AM60) are shown in Table 1 [7-9]. Composite specimens with 9%vol. $Al_2O_3$ fibres were prepared by a fibre preform casting process. The detailed information about the specific process can be found in references [10-12]. The unreinforced AM60 was also cast at the same condition. The rectangular samples were taken from the casting allowing sufficient surface area as required for the testing procedure.

Table 1 Thermoplysical properties of property of ceramic $Al_2O_3$ fibre [7-9]

| Material | $Al_2O_3$ fibre | AM60 |
|---|---|---|
| Elasticity modulus / GPa | 200 | 35-44 |
| Density /kg/m$^3$ | 3400 | 1740 |
| Diameter / μ m (average) | 4.0 | |
| Heat expansion coefficient /$10^{-6}$/K | 6 | 45 |
| Specific heat / J/(kg K) | 1000 | 1250 |
| Thermal conductivity / W/(m K) | 5 | 85 |

### Electrochemical experimentation

Electrochemical studies were carried out by using EC-LAB SP-150 electrochemical apparatus with corrosion analysis EC-lab software. A three-electrode cell was set up through assigning the samples as working electrode, Ag/AgCl/sat'd KCl electrode as a reference electrode and a Pt metal electrode as counter-electrode. At the beginning of experiments, samples were held in the salt solution allowing the open circuit potential to settle to a constant value. Potentiodynamic polarization scans were conducted at a rate of 10mv/s from -0.5v versus open circuit potential in a more noble direction up to 0.5v versus the reference electrode. Machined samples were ground with silicon carbide papers with various grades from 280 to 2500 grit, and then cleaned in acetone, rinsed with deionized water and dried prior to potentiodynamic polarization.

### Microstructural Analysis

Specimens were sectioned, mounted, and polished from the centre of cast cylindrical specimens with a diameter of 100mm and a height of 20mm and prepared following the standard metallographic procedures. A Buehler (Lake Bluff, IL) optical image analyzer 2002 system was used to determine the primary characteristics of the specimens. The detailed features of the microstructure were also characterized at high magnification using a JSM-5800LV (Tokyo, Japan) scanning electron microscope (SEM) with a maximum resolution of 100 nm in a backscattered model/l um in X-ray diffraction mapping mode, and maximum useful magnification of 30,000. To maximize the composition reading of the energy dispersive spectroscopy (EDS) data an etchant was applied to the polished specimens for microscopic examination.

## RESULTS AND DISCUSSION

### Microstructure

The cast microstructure of unreinforced AM60 alloy and 9 vol.% $Al_2O_3$ fibre-reinforced AM60 composite is depicted in Figures 1 and 2. From Figure 1, the microstructure analysis of the unreinforced AM60 indicates the presence of eutectic along the grain boundaries, within which the $\beta$-$Mg_{17}Al_{12}$ is present. The precipitates are hard and brittle and have certain contribution to the hardness values. Figure 2 illustrates that the short fibres are distributed in a random and isotropic orientation in the matrix alloy without agglomeration and caves.

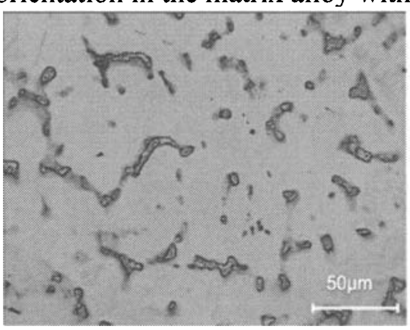


Figure 1 Optical photograph showing the microstructure of matrix AM60 alloy.

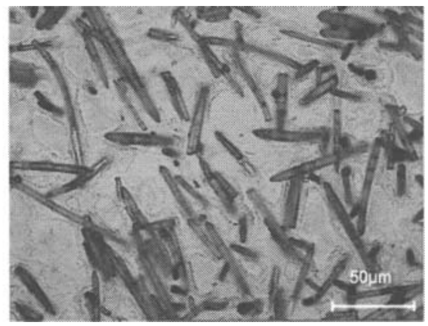


Figure 2 Optical photograph showing the microstructure of composite (9 vol% Fibres/ AM60).

Despite of the implication of a finer grain structure in the composite from Figures 1 and 2 resulting from the addition of fibres, it is difficult to distinguishthe difference in grain sizes between unreinforced AM60 alloy and $Al_2O_3$ fibre-reinforced AM60 composite. Thus, a common practice in the magnesium industry is to subject the as-cast specimens to a solution heat treatment (T4), which dissolves the $\beta$-$Mg_{17}Al_{12}$ phase and reveals the grain boundaries. Figure 3 distinctly reveals the grain boundaries of the unreinforced AM60 alloy and $Al_2O_3$ fibre-reinforced composites in the T4 condition. As can be seen, the grains in the matrix of the Fibre/AM60 composites are significantly refined compared with those of the AM60 alloy. Figure 4 presents the grain size measurements for both the unreinforced AM60 alloy and its composites. It is worth noting that the grain size of the AM60 alloy matrix is reduced to around 50μm in the composites due to the grain refinement effect of the fibres.

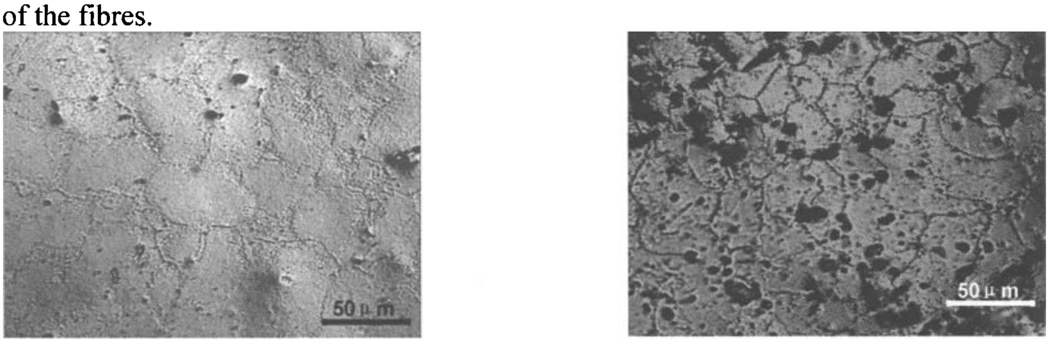


(a) (b)

Figure 3 Optical micrograph showing grain structure of (a) AM60 alloy and (b) Fibre/AM60 in T4 condition

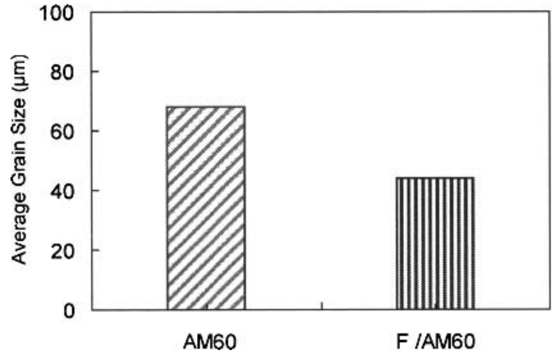


Figure 4 Measured grain size of the matrix alloy and F/AM60.

It is evidently observed from Figure 5 that the eutectic phases attach to the surface of the reinforcement. This observation indicates that the eutectic phases are able to wet $Al_2O_3$ fibres. As a result, they can heterogeneously nucleate on the substrate of $Al_2O_3$ fibres, and grows on the reinforcement. The heterogeneous nucleation of the eutectic phase on reinforcement may be attributed to the relationship of coherent interface between the eutectic phase and the reinforcement. .

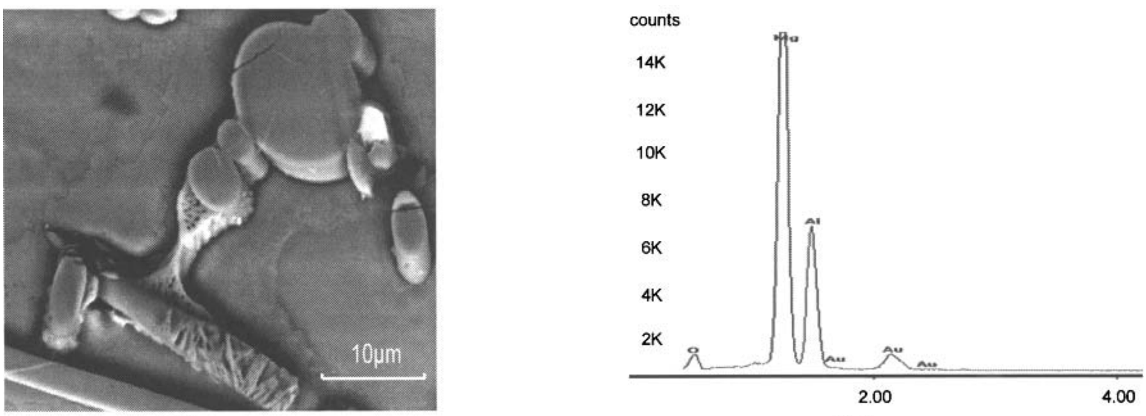


(a) (b)

Figure 5 Fibre serve as nucleation of eutectic phase, (a) Arrow A-fibre is heterogeneous nucleation substrate and (b) EDS result of Al-Mg eutectic phases in Fibre/AM60 composites

Comparing the microstructure of the composite with that of the alloy, it is obvious that, the role of alumina fibers in the microstructure development of the composite is to refine grain structure in the magnesium alloy matrix. Due to the presence of the eutectic phases adjacent to the reinforcement, on the other hand, Al content around the alumina fiber is higher than that of the original alloy matrix. This is because the bulk analysis shows the eutectic phase contains 30-36 wt. % Al compared with 6 wt.% Al in average in the matrix magnesium alloy.

Potentiodynamic Polarization

Potentiodynamic testing results yields the polarization curves shown in Figures 6 and 7 for the 1wt% and 3.5wt% NaCl solutions, respectively. The corrosion potentials, corrosion current density, and anodic/cathodic Tafel slopes ($\beta_A$ and $\beta_C$) were derived from the test data. Based on the approximately line polarization at the corrosion potential ($E_{corr}$), the polarization resistance ($R_p$) values were determined from the relationship [13, 14]:

$$R = \frac{\beta_A \beta_C}{2.303\, i_{corr}(\beta_A + \beta_C)}$$

where $i_{corr}$ is the corrosion current density. A summary of the results of the potentiodynamic corrosion tests is given Table 2.

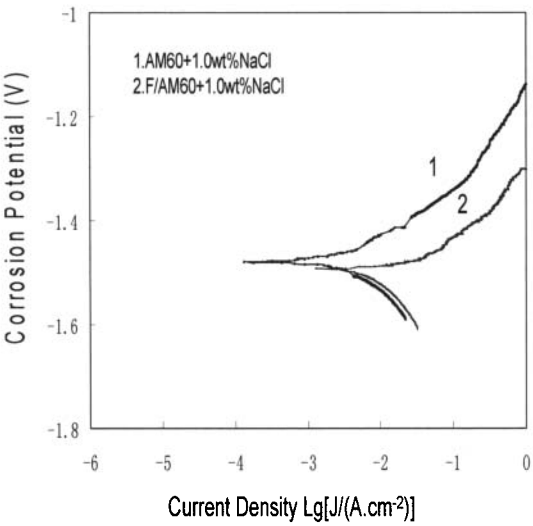


Figure 6 Potentiodynamic polarization curves for of the $Al_2O_3$ fiber/AM60 composites and its pure matrix alloy in 1.0wt% NaCl solution.

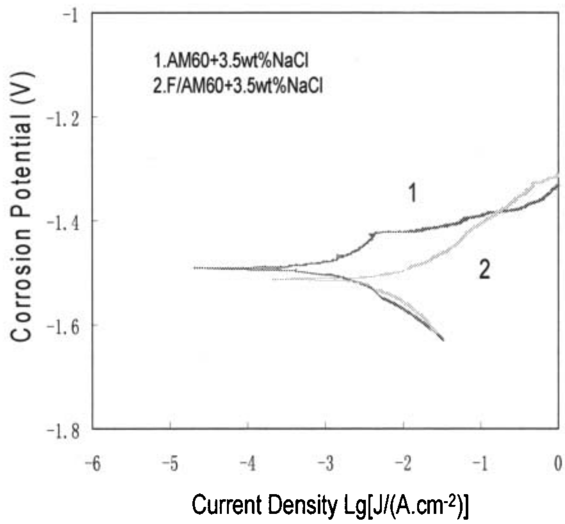


Figure 7 Potentiodynamic polarization curves for of the $Al_2O_3$ fiber/AM60 composites and its pure matrix alloy in 3.5wt% NaCl solution.

Table 2 Summary of polarization curve characteristics and calculated polarization resistance

| | Materials type | $I_{pitting}$($\mu$A/cm$^2$) | $E_{pitting}$(V) | $I_{corr}$($\mu$A/cm$^2$) | $E_{corr}$(V) | R(k$\Omega$.cm$^2$) |
|---|---|---|---|---|---|---|
| 1% | AM60 | 14.9 | -1.413 | 4.888 | -1.4778 | 5.06 |
| NaCl | $Al_2O_3$ fiber/AM60 | N/A | N/A | 7.028 | -1.4959 | 1.28 |
| 3.5% | AM60 | 4.44 | -1.423 | 1.038 | -1.4912 | 12.9 |
| NaCl | $Al_2O_3$ fiber/AM60 | N/A | N/A | 6.42 | -1.5137 | 2.82 |

The main differences in corrosion behavior between the compositeand matrix alloy are illustrated in Figures 6 and 7. The composite as compared with matrix alloy, shifts the polarization curves to higher current densities, and consequently become more active than matrix alloy and more noticeable in the stronger salt solution. The polarization resistance ($R_p$) of composite is decreased by 5 times (Table 2) than that of matrix alloy. In both solutions, $R_p$ is decreased by the addition of $Al_2O_3$ fibers and the values of composites are much lower than those of matrix alloy. In general, the parameter ($E_{pit}$-$E_{corr}$) is used to measure the extent of the passive region on the polarization curves. Given in Figures 6 and 7, all curves exhibit a different regime for the matrix alloy and composites. The results indicate the onset of pitting is not visible for the composites, which means that $E_{pit}$ is very close to $E_{corr}$, compared with a well-defined pitting potential for matrix alloy. It is known that galvanic corrosion is the primary prospect when active magnesium is coupled with a relatively noble material [13]. But, no galvanic interaction between the alloy matrix and reinforcing fiber could take place since the $Al_2O_3$ fiber is an insulator. Hypothetically, it implies that the addition of $Al_2O_3$ fiber to the AM60 alloy should increase the corrosion resistance of the composite. However, the introduction of fiber reinforcements into the matrix alloy indeed generates new interfaces between the Mg matrix and $Al_2O_3$ fiber . The presence of Mg matrix/ $Al_2O_3$ fiber interfaces breaking the continuity of the Mg matrix and creating preferential locations for corrosion attack, and consequently decreases corrosion resistance of the composite. This type of corrosion was observed in $SiC_p$/ZC71 composites by Nunez-lopez [15].

## CONCLUSIONS

- The addition of alumina fibers leads to a significant refinement in the grain size, which are 50 μm and 68 μm for fiber reinforced composites and matrix magnesium alloy, respectively.
- it containing The high Al-containing zones is present adjacent to the alumina fiber compared to Al content in the original alloy matrix since fibers serves as heterogeneous nucleation sites for the eutectic phase.
- Electrochemical testing results show that the presence of alumina fibers deteriorates the corrosion resistance of magnesium. The magnesium matrix alloy exhibits a higher corrosion resistance value (5.06 $k\Omega.cm^2$ and $12.9k\Omega.cm^2$ in 1.0wt% and 3.5wt% NaCl solution, respectively) than the fiber reinforced composites (1.28 $k\Omega.cm^2$ and $2.82k\Omega.cm^2$ in 1.0wt% and 3.5wt% NaCl solution, respectively).

## ACKNOWLEDGEMENTS

The authors would like to take this opportunity to thank the Natural Sciences and Engineering Research Council of Canada and University of Windsor for financially supporting this work.

## REFERENCES

[1] H. Ye, and X. Liu, Review of recent studies in magnesium matrix composites, Journal of materials science, (39), 2004, 6153-6171.
[2] J. Yao, W. Wang, and L. Fang, Morphology of the wear surface and sub-surface of net work ceramic reinforced aluminum matrix composites, Special Casting& Nonferrous alloy, (4), 2001, 5-9.
[3] M. Zhou, H. Hu, N. Li and J. Jo, Microstructure and tensile properties of squeeze cast magnesium alloy AM50, Journal of materials engineering and preformance, (14), 2005, 539-545.
[4] J. Lo, and R. Santos, Magnesium matrix composites for elevated temperature applications, 2007 SAE World Congress, SAE, Detroit, MI, 2007-01-1028.
[5] Q. Zhang, and H. Hu, Processing and Characterization of Al-based Hybrid Composites, EPD 2009, TMS, 2009, 769-775.
[6] H.Umehara, M.Takaya, Corrosion Resistance of Die Casting AZ91D Magnesium Alloys in the Atmosphere, Magnesium Alloys and Their Applications, Wiley-Vch, Germany, 2000, 506-513.
[7] D.R. Poirier, G.H.Geiger, Transport phenomena in Materials processing, TMS, USA, 1994.
[8] Magnesium and Magnesium Alloys, ASM Specialty Handbook, the Materials Information Society, USA, 1999.
[9] J. A. Dicarlo, High temperature structural fibers- status and needs, NASA .Technical memorandum 105174, May 1991.
[10] Qiang Zhang, Master thesis, University of Windsor, Ontario, Canada, 2009.
[11] Q. Zhang, and H. Hu, Development of Hybrid Magnesium-based Composites, Magnesium for Automotive Applications, 2010 SAE World Congress &Exposition, 2010, Detroit, USA.
[12] Q. Jing, Solidification microstructures in a short fiber reinforced alloy composite containing different fiber fractions, China Foundry. Vol.3, No.1, Feb 2006.
[13] M.G.Fontana, Corrosion Engineering, 3th ed., McGraw-Hill International Edition, 1996, 42.
[14] M.S.Phadke, Quality Engineering of Robust Design, AT&T Bell Laboratory, NY, USA, 1989.
[15] C.A.Nunez-lopez, The Corrosion Behaviour of Mg Alloy ZC71/SiCp Metal Matrix Composites, Corrosion Science, Vol.37, No.5, 1995, 689-708.